View Article Online
View Journal

Dalton Transactions

An international journal of inorganic chemistry

Accepted Manuscript

This article can be cited before page numbers have been issued, to do this please use: K. M. Kowalski, . Szczupak, A. Kowalczyk, D. Trzybiski, K. Wozniak, G. Mendoza, M. Arruebo, D. Steverding and P. Stczek, *Dalton Trans.*, 2019, DOI: 10.1039/C9DT03948A.

This is an Accepted Manuscript, which has been through the Royal Society of Chemistry peer review process and has been accepted for publication.

Accepted Manuscripts are published online shortly after acceptance, before technical editing, formatting and proof reading. Using this free service, authors can make their results available to the community, in citable form, before we publish the edited article. We will replace this Accepted Manuscript with the edited and formatted Advance Article as soon as it is available.

You can find more information about Accepted Manuscripts in the Information for Authors.

Please note that technical editing may introduce minor changes to the text and/or graphics, which may alter content. The journal's standard Terms & Conditions and the Ethical guidelines still apply. In no event shall the Royal Society of Chemistry be held responsible for any errors or omissions in this Accepted Manuscript or any consequences arising from the use of any information it contains.

Organometallic ciprofloxacin conjugates with dual action: synthesis, characterization, and antimicrobial and cytotoxicity studies

View Article Online
DOI: 10.1039/C9DT03948A

Łukasz Szczupak[1,†], Aleksandra Kowalczyk[2,†], Damian Trzybiński[3], Krzysztof Woźniak[3], Gracia Mendoza[4], Manuel Arruebo[4,5], Dietmar Steverding[6], Paweł Stączek[2,*], and Konrad Kowalski[1,*]

[1]Faculty of Chemistry, Department of Organic Chemistry, University of Łódź, Tamka 12, 91-403 Łódź, Poland; kondor15@wp.pl and konrad.kowalski@chemia.uni.lodz.pl (K.K.); lukasz.szczupak@chemia.uni.lodz.pl (Ł.S.)

[2] Department of Microbial Genetics, Faculty of Biology and Environmental Protection, University of Łódź, Banacha 12/16, 90-237 Łódź, Poland; aleksandra.strzelczyk@biol.uni.lodz.pl (A.S.); pawel.staczek@biol.uni.lodz.pl (P.S.)

[3]Faculty of Chemistry, Biological and Chemical Research Centre, University of Warsaw, Żwirki i Wigury 101, 02-089 Warszawa, Poland; trzybinski@chem.uw.edu.pl (D.T.); kwozniak@chem.uw.edu.pl (K.W.)

[4]Department of Chemical Engineering., University of Zaragoza, Campus Río Ebro-Edificio I+D, C / Poeta Mariano Esquillor S / N, 5018 Zaragoza, Spain; Aragon Health Research Institute (IIS Aragón), 50009 Zaragoza, Spain; arruebom@unizar.es (M.A.); gmmenc@unizar.es (G.M.)

[5]Networking Research Center on Bioengineering, Biomaterials and Nanomedicine, CIBER-BBN, 28029 Madrid, Spain

[6]Bob Champion Research & Education Building, Norwich Medical School, University of East Anglia, Norwich Research Park, Norwich NR4 7UQ, UK; D.Steverding@uea.ac.uk (D.S.)

† These authors contributed equally to work*Correspondence to: konrad.kowalski@chemia.uni.lodz.pl and kondor15@wp.pl; Tel.: +48-42-635-5759 and pawel.staczek@biol.uni.lodz.pl; Tel.: +48 -42-635-4466

View Article Online
DOI: 10.1039/C9DT03948A

ABSTRACT

The synthesis, characterization and biological activity of six bioorganometallic conjugates of ciprofloxacin with ferrocenyl, ruthenocenyl and cymantrenyl entities is described. Their antimicrobial activities were investigated against Gram-positive bacteria, Gram-negative bacteria and bloodstream forms of *Trypanosoma brucei*. Furthermore, morphological changes of bacterial cells upon treatment with the conjugates were examined by scanning electron microscopy. In addition, the cytotoxicity of the conjugates against tumor and normal mammalian cells was also investigated. The results showed that conjugation of an organometallic moiety can significantly enhance the antimicrobial activity of the antibiotic ciprofloxacin drug. It was found that *N*-alkyl cymantrenyl and ruthenocenyl ciprofloxacin conjugates were the most effective derivatives although other conjugates showed also significant antimicrobial activity. The increase in antimicrobial activity was most likely due to two independent mechanisms of action. The first mechanism is due to the bacterial topoisomerase inhibitory activity of ciprofloxacin while the second mechanism can be attributed to the generation of reactive oxygen species caused by the organometallic moiety. The presence of two modes of action enables the conjugates to kill bacteria in their stationary growth phase and to overcome drug resistance of *S. aureus* strains. In addition, the conjugates showed promising selectivity toward bacterial and parasite cells over mammalian cells.

View Article Online
DOI: 10.1039/C9DT03948A

Introduction

Organometallic derivatization (or conjugation) of medicinally important molecules like drugs, drug leads or natural products has been shown to be an efficient method for obtaining new therapeutic and diagnostic agents.[1-10] A major impetus into the research of organometallic compounds has been the development of anticancer agents. For instance, ferrocenyl derivatives of the anti-breast cancer drug tamoxifen are key examples of this group.[11] Far less attention has been given towards the development of organometallic antibacterial and antiparasite drug derivatives. This field of research is, however, increasingly important due to the worldwide spread of drug-resistant bacteria and an urgent need for new antiparasite drugs.[12-18] Seminal report on ferrocenyl (Fc) derivatives of β-lactam antibiotics have been published in the 1970s.[19] Recently, our group reported on Fc and ruthenocenyl (Rc) derivatives of 6-aminopenicillinic acid (6-APA) and 7-aminodesacetoxycephalosporanic acid (7-ADCA).[20-23] Several atomic resolution X-ray crystal structures of the ruthenocenyl β-lactam derivatives complexed with bacterial CTX-M β-lactamase were solved providing structural insight into the mode of binding of the conjugates to the enzyme active site.[21-23] Further, recent examples of organometallic derivatives of well-established antibacterial drugs or therapeutically promising antibiotics comprise ferrocenyl derivatives of novobiocin[24] or ferrocenyl, cymantrenyl and half-sandwich chromium platensimicin derivatives.[25,26] Other examples of organometallic antiparasite drug derivatives include antimalarial ferroquine,[27,28] manganese(I) tricarbonyl complexes of ketoconazole, miconazole and clotrimazole,[29] antimalarial ferrocenyl quinolones,[30] cymantrene and cyrhetrene chloroquines,[31] antischistosomal Cr tricarbonyl praziquantel drug derivatives,[32] and ferrocenyl derivatives of the anthelmintic drug monepantel.[33]

Quinolones are synthetic antibacterial drugs with broad-spectrum activity against Gram-positive and Gram-negative pathogenic strains. They are the only class of synthetic antibacterial drugs competing with β-lactam antibiotics in terms of effectiveness and worldwide clinical use. The story of quinolones started with the discovery of nalidixic acid in 1962.[34] Since then, many generations of quinolones have been introduced into the market with norfloxacin,[35] ofloxacin,[36] ciprofloxacin,[37] sitafloxacin,[38] and nadifloxacin[39] as relevant examples.

Quinolones cross the bacterial cell wall by passive diffusion, which is a major up-take mechanism in Gram-positive strains, and by porin-mediated influx mechanisms in Gram-negative strains.[40] Quinolones are bacterial topoisomerases inhibitors.[41] Topoisomerase inhibition has been, for a long time, considered

as a sole mechanism of quinolones bactericidal activity. However, recent reports showed that this mechanism is accompanied by the ability of quinolones to generate reactive oxygen species (ROS) in bacterial cells.[42,43] Bacterial DNA gyrase and DNA topoisomerase IV belong to the type II DNA topoisomerase family and they are validated targets for quinolone antibacterial therapy.[41,44] Both of these enzymes change bacterial chromosome topology by transient double-strand DNA scission, a change of the DNA linking number, and subsequent covalent linking of the cleaved strands.[45,46] All topoisomerases can relax supercoiled DNA, but only DNA gyrase can also introduce negative supercoils in a reaction that require the hydrolysis of ATP.[47] Bacterial topoisomerases II consist of A and B subunits which must aggregate to form an A_2B_2 active tetramer complex. XRD molecular structures of gyrase-fluoroquinolones adducts have been reported,[48,49] indicating that quinolones do not bind to either DNA or topoisomerase enzyme alone. Instead, they bind to the DNA-A_2B_2 complex targeting the DNA-cleavage active site positioned at the *DNA gate* of the enzyme. This mode of binding hinders effective DNA religation and results in lethal DNA double-strands breaks.[50] The clinical success of quinolones came with the price of the emergence of bacterial resistance to this class of drugs.[51] To address this problem, there is a need of quinolones with activity against drug-resistant clinical isolates of pathogenic bacterial strains.

Here we describe the preparation of six organometallic ciprofloxacin (**CIP**) derivatives bearing either ferrocenyl (**1**,**4**), ruthenocenyl (**2**,**5**) or cymantrenyl (**3**,**6**) moieties and the biological activities of these compounds. The compounds were tested for their activity against a panel of Gram-positive and Gram-negative laboratory and clinical bacterial strains. There is evidence that common different classes of antibiotics (*e.g.,* fluoroquinolones and β-lactams) act as ROS generating agents[52] and that the oxidative stress (OS) triggered by these antibiotics contributes to their antibacterial activity[43] and toxicity.[52] Because of this we also investigated the organometallic ciprofloxacin derivatives for their ability to generate ROS in bacteria and attempted to correlate the ROS production with the antibacterial activity of the compounds. In addition, we report on inhibitory activity studies of **1-6** towards bacterial gyrase and topoisomerase IV. We also evaluated the antitrypanosomal activity of **1-6** against the protozoan parasite *Trypanosoma brucei*. Furthermore, the effect of compounds **4**, **5** and **6**, as well as ciprofloxacin (**CIP**), on the morphology of *E. coli* and *S. aureus* was studied by scanning electron microscopy (SEM).

Results and discussion

Synthesis

View Article Online
DOI: 10.1039/C9DT03948A

Two groups of organometallic ciprofloxacin (**CIP**) derivatives were obtained as depicted in Scheme 1. In both groups the organometallic-spacer moiety substitutes the hydrogen atom of the piperazin-1-yl ring in **CIP**. Compounds **1-3** are *N*-acyl and **4-6** are *N*-alkyl derivatives, respectively. Derivatives **1-3** were obtained in reaction of **CIP** with the appropriate carboxylic acid **A**, **B** or **C** in dichloromethane in the presence of 1-ethyl-3-(3-dimethylaminopropyl)carbodiimide hydrochloride (EDC-HCl) and 4-(dimethylamino)pyridine (DMAP) (Scheme 1). Compounds **4-6** were obtained by a one-pot, two-step process developed in our group consisting of dehydrohalogenation of compounds **D-F** followed by a Michael addition reaction of *in situ* generated acryloyl-intermediates with ciprofloxacin.[53]

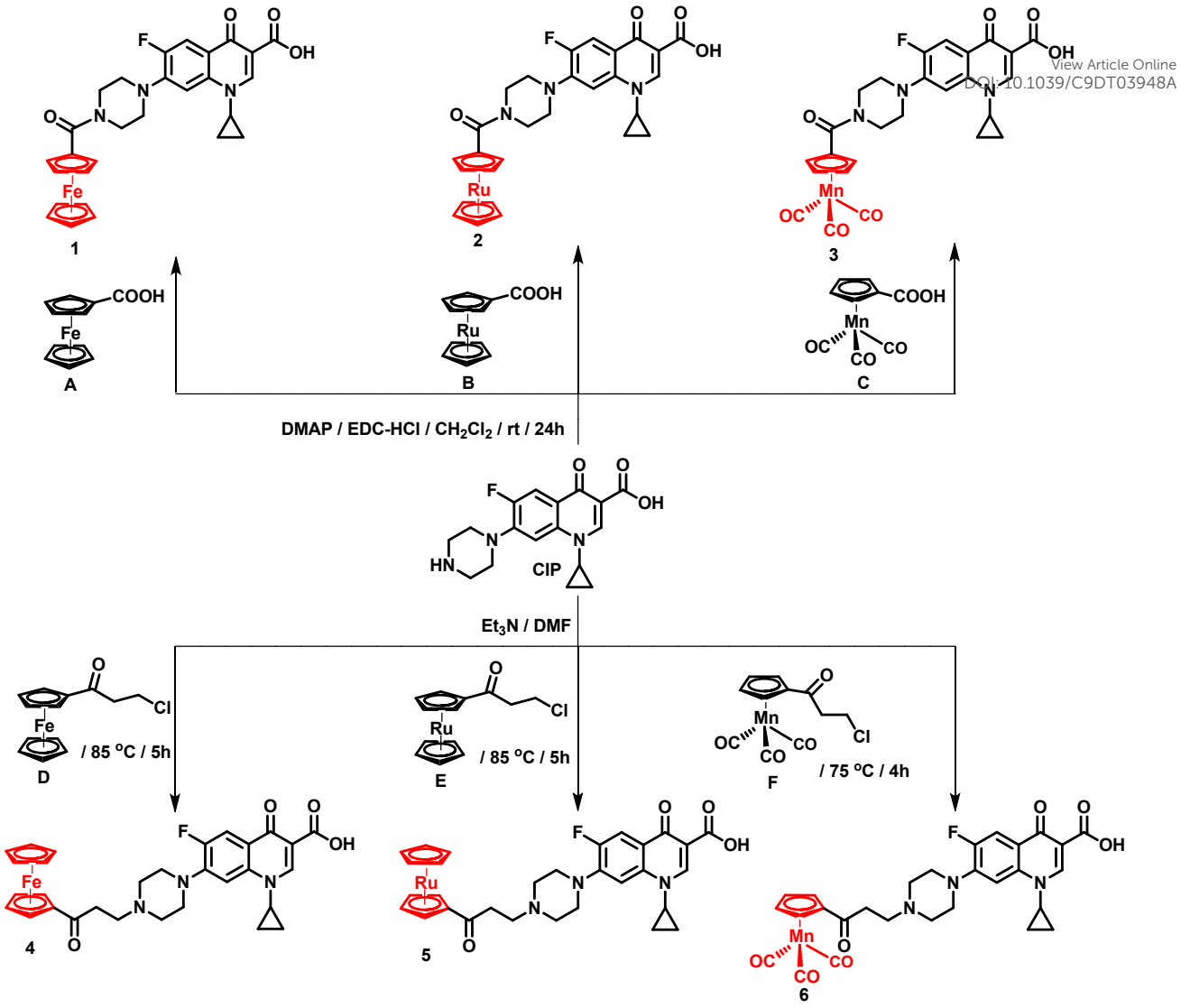

Scheme 1 Synthesis of organometallic ciprofloxacin conjugates **1-6**

Ciprofloxacin derivatives **1-6** were isolated as crystalline solids in 80, 51, 52, 80, 87, and 85% yields, respectively. All compounds were characterized by ^{1}H, ^{13}C-NMR, IR spectroscopy, mass spectrometry and elemental analyses. The ^{1}H NMR spectra of **1-6** are shown in Figs. S1-S6 (ESI). The obtained analytical data confirmed the proposed structures. In addition, the structure of **4** and **6** in solid state was determined by single-crystal X-ray structural analysis.

X-ray structure determination

Crystals of **4** and **6** suitable for single-crystal X-ray diffraction structure determination were obtained by slow diffusion of *n*-pentane into a 1,2-dimethoxyethane solution of **4** and into a chloroform solution of **6**, respectively. The crystal and structure refinement data are presented in Table S1. The molecular structure of **4** and **6** are shown in Figure 1 and 2, together with selected geometrical parameters. Full list of bond distances (Å), valence and torsion angles (°) are listed in Tables S2-S7.

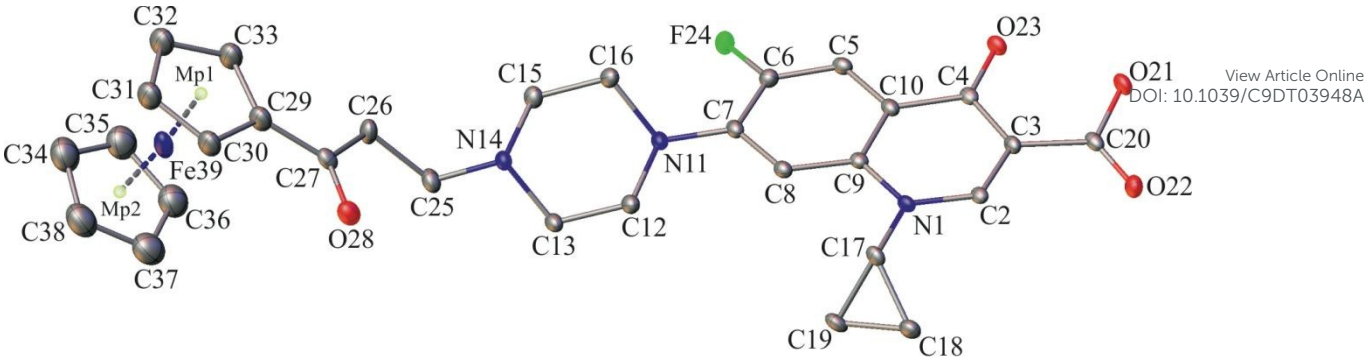

Fig. 1 Molecular diagram of **4** with atomic displacement ellipsoids at the 25% probability level; Mp_1 and Mp_2 correspond to mid-points of the substituted and unsubstituted cyclopentadienyl rings, respectively. Selected bond lengths [Å] and angles [°]: Mp_1−Fe, 1.659(4); Mp_2−Fe, 1.632(2); Fe39−C29, 2.033(7); Fe39−C30, 2.063(8); Fe39−C36, 2.030(7); C29−C27, 1.466(9); C26−C25, 1.514(8); C30−C29, 1.430(9); O28−C27, 1.229(7); O21−C20, 1.339(7); O22−C20, 1.209(7); N14−C25, 1.471(7); N1−C17, 1.456(6); F24−C6, 1.361(6); C32−C33−C29, 106.8(6); O28−C27−C26, 121.3(6); N14−C25−C26, 121.3(6); N14−C25−C26, 114.2(5); C30−C29−C33−C32, 0.6(9); C26−C27−C29−C30, 170.3(7).

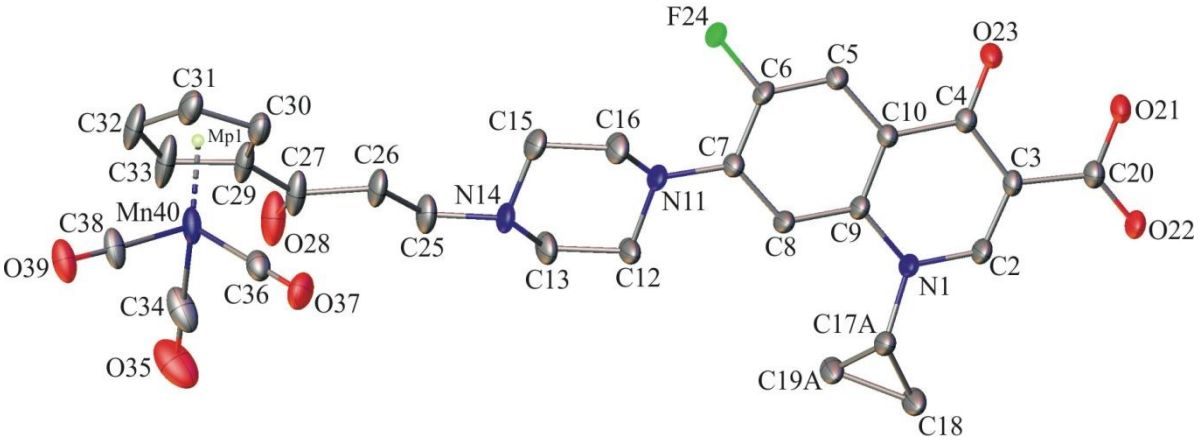

Fig. 2 Molecular diagram of **6** with atomic displacement ellipsoids at the 25% probability level; Mp_1 corresponds to mid-point of the cyclopentadienyl ring. Selected bond lengths [Å] and angles [°]: Mp_1−Mn40, 1.759(3); Mn40−C29, 2.118(5); Mn40−C36, 1.793(5); C29−C27, 1.498(7); C26−C25, 1.526(6); C30−C29, 1.403(8); O28−C27, 1.198(8); O21−C20, 1.319(5); O22−C20, 1.212(5); N14−C25, 1.470(6); N1−C17, 1.492(8); F24−C6, 1.365(4); C32−C33−C29, 107.2(6); O28−C27−C26, 122.0(5); N14−C25−C26, 113.2(5); C30−C29−C33−C32, 0.2(8); C26−C27−C29−C30, -0.4(9).

Compound **4** and **6** both crystalized in the monoclinic space group, ferrocene derivative **4** in the *C*2/*c* and cymantrene derivative **6** in the $P2_1/c$. The single-crystal X-ray structure analysis confirmed postulated structures in which the organometallic moiety was bound to the nitrogen atom of the piperazin-1-yl group. The iron atom in **4** was symmetrically located between the cyclopentadienyl (Cp) rings with a

distance of 1.659(4) Å and 1.631(2) Å to the midpoints of each cyclopentadienyl ring (Mp_1 and Mp_2, respectively). The ferrocenyl moiety in **4** deviated from the staggered conformation by about 10°. The manganese atom in **6** was bonded to the Cp ligand and to the three carbonyl ligands. This is the typical molecular architecture of cymantrenyl three-legged piano-stool derivatives.[54] In the crystal lattice, individual molecules of either, **4** or **6** were involved in intramolecular C−H···O and C−H···F hydrogen bonds and in the network of weak π- π and C−F···π contacts (Fig. S7 and S8, Table S8-S13). Of notice is that the crystal lattice of **6** contained solvent accessible voids running along the crystallographic *b*-direction (Fig. S8, voids are marked in yellow).

Antibacterial activity

The antibacterial activity of compounds **1-6** and their commercially available metallocene precursors (ferrocene carboxylic acid **A**, ruthenocene carboxylic acid **B**, and cymantrene carboxylic acid **C**) was tested against a set of reference Gram-negative strains (*Escherichia coli* ATCC 25922, *E. coli* NCTC 8196, *Proteus vulgaris* ATCC 49990, *Klebsiella pneumoniae* ATCC 13883*)* and Gram-positive strains (*Staphylococcus aureus* ATCC 6538, *S. aureus* ATCC 29213, *Staphylococcus epidermidis* ATCC 12228), and additionally against two clinical bone isolates of methicillin-resistant *S. aureus* (MRSA) as well as against *S. aureus* ATCC 6538 CIP^R, a mutant strain resistant to high concentrations of **CIP** (>60 x MIC) that was obtained in our laboratory through selection using increasing concentrations of the antibiotic on agar plates. All three tested metallocene precursors did not have any antibacterial activity within the tested concentrations of 0.2 – 200 μM (data not shown). The antibacterial activity of **1-6** are shown in Table 1 as minimal inhibitory concentration (MIC) values. In general, compounds **4-6** showed higher antibacterial activity against all strains tested compared to their congeners **1-3**. Noticeably, compounds **5** and **6** were more active against *E. coli* ATCC 25922 strain than **CIP**. Their MIC values were 0.0006 and 0.0001 μM, respectively, while the MIC of **CIP** was 0.01 μM. It means that in the case of **6**, the MIC value was 100 times lower than that of **CIP**. Furthermore, compound **6** was more active than **CIP** against *S. aureus* ATCC 6538 and *K. pneumoniae* ATCC 13883 with MICs of 0.4 and 0.001 μM, respectively. In the former case, the MIC value of **6** was 50 times lower than that of **CIP**. Compounds **5** and **6** were also highly active against all Gram-positive strains with similar MIC values as **CIP**. The most active compounds of **1-3** series was the cymantrenyl derivative **3**. It showed better antibacterial activity against both D15 and D17 MRSA strains than **CIP** with MIC values of 0.8 μM, and thus was 4 times more active than **CIP**. It should be noted that both clinical isolates showed reduced susceptibility to **CIP**. Interestingly, the same four-fold increase in potency of compound **3** over **CIP** was also observed for the **CIP** resistant *S. aureus* 6538 CIP^R strain, despite the fact that the MIC values of both drugs were greater than those for the wild type strain. As antibacterial drugs can be either bacteriostatic (inhibition of growth) or bactericidal (killing of bacteria), we determined also a minimal

bactericidal concentration (MBC) for compounds **1-6** (Table 1). The MBC values for the most active compounds **5** and **6** against *E. coli* ATCC 25922, and **6** against *K. pneumoniae* were approximately 10 times and 5 times lower, respectively, than those obtained for **CIP** against these strains. However, the MBC/MIC ratio was > 4, which indicates more bacteriostatic rather than bactericidal activity.[55] In the case of the other strains where the MIC values of these compounds were similar to that of **CIP**, the compounds showed predominantly bactericidal activity (MBC/MIC ratio < 4, Table 1). Predominant bactericidal mode of activity was also observed for all other compounds.

Table 1 Minimal inhibitory concentration (MIC in μM) and minimal bactericidal concentration (MBC, in μM) of **1-6** and **CIP** against panel of Gram-negative and Gram-positive bacterial strains. CIP^R-resistant to high concentration of **CIP**

strain	Antibacterial activity [μM]													
	1		**2**		**3**		**4**		**5**		**6**		**CIP**	
	MIC	MBC	MIC	MBC	MIC	MBC	MIC	MBC	MIC	MBC	MIC	MBC	MIC	MBC
E.coli ATCC 25922	6.2	>25	6.2	>25	6.2	25	0.08	0.08	0.0006	0.005	0.0001	0.005	0.01	0.04
E.coli NCTC 8196	25	>25	25	>25	12.5	25	0.4	0.4	0.04	0.08	0.04	0.04	0.04	0.08
P.vulgaris ATCC 49990	na	nd	na	nd	na	nd	1.6	1.6	3.1	6.2	0.2	0.2	0.1	0.2
K.pneumoniae ATCC 13883	na	nd	na	nd	25	>25	0.2	0.4	0.05	0.2	0.001	0.01	0.05	0.05
S.aureus ATCC 6538	6.2	25	6.2	25	0.8	3.1	3.1	6.2	0.8	1.6	0.4	3.1	0.8	1.6
S.aureus ATCC 29213	6.2	12.5	6.2	25	0.8	1.6	3.1	6.2	1.6	1.6	0.8	1.6	0.4	1.6
S.epidermidis ATCC 12228	12.5	12.5	12.5	>25	1.6	1.6	1.6	3.1	0.8	1.6	0.8	0.8	0.4	0.8
S.aureus D15 (MRSA)	6.2	12.5	6.2	12.5	0.8	1.6	6.2	6.2	3.1	6.2	3.1	6.2	3.1	3.1
S.aureus D17 (MRSA)	6.2	25	6.2	>25	0.8	3.1	6.2	12.5	3.1	6.2	3.1	12.5	3.1	6.2
S. aureus CIP^R	nd	nd	nd	nd	12.5	50	50	>50	50	>50	50	>50	50	>50

na – no activity, nd – not determined

The influence of *N*-acetyl-L-cysteine (NAC) on antibacterial activity

There is a growing evidence that some antibiotics, in addition to their individual activity against a specific target, have also the ability to produce reactive oxygen species (ROS). The mechanism of ROS production involves the activation of the tricarboxylic acid (TCA) cycle followed by hyper-induction of the electron transport chain.[43, 56-58] In order to assess whether ROS production played a role in the antibacterial activity of our organometallic ciprofloxacin derivatives, we studied the antibacterial

activity of the three most active compounds **3**, **5**, and **6** in the presence of the free radical scavenger *N*-acetyl-L-cysteine (NAC) against *E. coli* ATCC 25922 and *S. aureus* ATCC 6538 strains (Table 2).

View Article Online
DOI: 10.1039/C9DT03948A

Table 2 Antibacterial activity of **3**, **5**, **6** and **CIP** in the presence of 10 mM *N*-acetyl-l-cysteine (NAC) antioxidant after 24 h treatment expressed as MIC_{NAC} [μM] and $[MIC_{NAC}]/MIC$ ratio where $[MIC_{NAC}]$ is a value of MIC determined in the presence of the antioxidant

	MIC_{NAC} [μM]				$[MIC_{NAC}]/MIC$ [ratio]			
	3	**5**	**6**	**CIP**	**3**	**5**	**6**	**CIP**
***E.coli* ATCC 25922**	6.2	0.6	0.3	0.16	1	1000	3000	16
***S. aureus* ATCC 6538**	6.2	6.2	6.2	6.2	7.75	7.75	15.5	7.75

In the case of the *E. coli* strain, a significant increase in the MIC value was observed for compounds **5** and **6** and for **CIP** in the presence of NAC (Table 2). The $[MIC_{NAC}]/MIC$ ratio for **5** and **6** was greater than 1000 while that for CIP was only 16. For compound **3**, which had a much higher MIC value against *E. coli* ATCC 25922, the effect of NAC was negligible. For the *S. aureus* strain, a similar increase in the MIC value was observed for all three compounds and **CIP**. However, the effect was less pronounced and the $[MIC_{NAC}]/MIC$ ratio was only moderate (Table 2). Nevertheless, these results indicate that ROS seem to play a role in the mode of antibacterial action of compounds **3**, **5**, and **6**.

Antibacterial activity in stationary phase

Most bactericidal antibiotics require bacteria to be actively dividing in order to exhibit their killing activity. However, in many infections, depending on their stage, bacteria divide very slowly if at all (stationary phase) and form biofilms. Moreover, some cells in these biofilms are so called peristers, which have a significantly reduced metabolism and tend to have acquired temporary antibiotic-resistant phenotypes.[59, 60, 61] Therefore, compounds with the ability to kill bacteria in their stationary growth phase are especially sought-after. For this reason, we studied the antibacterial activity of compounds **4**, **5,** and **6** against *E. coli* ATCC 25922, and **3,** and **6** against *S. aureus* ATCC 6538 in their stationary growth phase.

View Article Online
DOI: 10.1039/C9DT03948A

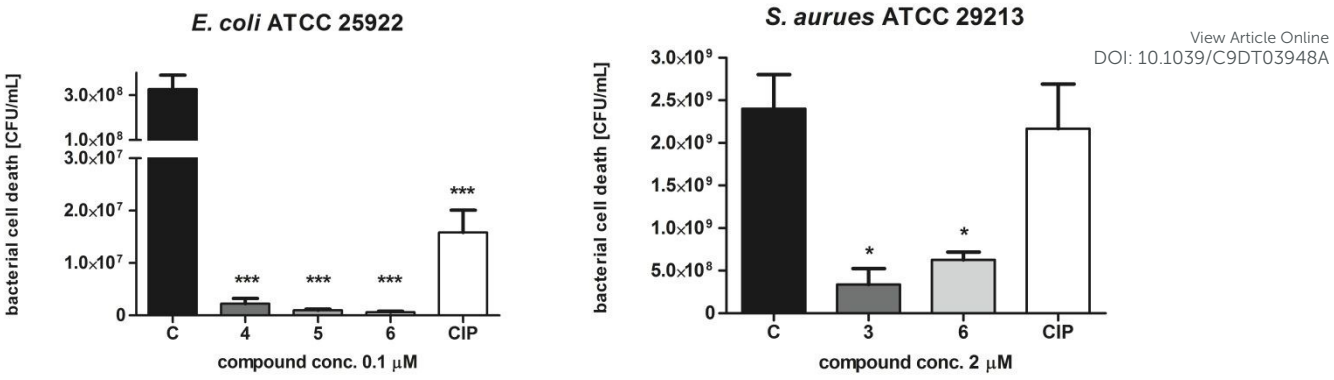

Fig. 3 Bactericidal effect of organometallic ciprofloxacin derivatives observed after 24 h exposure of stationary-phase *E. coli* and *S. aureus* cells. Compounds **4, 5, 6,** and **CIP** were tested at 0.1 μM against *E. coli* and compounds **3**, **6,** and **CIP** at 2 μM against *S. aureus.* Prior to treatment with the compounds, cultures were grown for 24 h to generate high cell density stationary-phase batches. The results were expressed as means ± SEM from three independent experiments (n = 3). Comparisons between compounds and untreated control (**C**) were made using One-way ANOVA analysis of variance (* $P<0.05$, *** $P<0.001$).

All three organometallic ciprofloxacin derivatives **4**, **5,** and **6** resulted in a statistically significant decrease in the viability of stationary-phase *E. coli* cells compared to the untreated control (Fig. 3). The highest bactericidal activity showed compound **6**, resulting in a decrease in cell viability from 3.3 x 10^8 to 2.2 x 10^6 CFU/mL, followed by compound **5** and **4**, which perfectly coincided with the MICs pattern for exponentially growing bacteria. **CIP** also caused a statistically significant decrease in bacterial viability, however, it was about 10 times less potent than the organometallic ciprofloxacin derivatives (decrease from 3.3 x 10^8 to 1.6 x 10^7 CFU /mL).

Bactericidal activity on stationary-phase *S. aureus* cells was evaluated with compounds **3** and **6**, which had the lowest MIC values against exponentially growing *staphylococci* (see above). Both compounds caused a statistically significant decrease in the viability of the bacteria compared to the untreated control (from 2.4 x 10^9 to 3.4 x 10^8 CFU/mL for **3**, and 6.3 x 10^8 CFU/mL for **6**). In contrast, **CIP** did not show bactericidal activity at the tested concentration against *S. aureus* in the stationary growth phase.

As fluoroquinolones such as **CIP** require cell activity (replication, transcription) to establish their bactericidal activity,[51, 62] it can be hypothesized that our new organometallic ciprofloxacin derivatives seem to have, in addition to their ability to inhibit topoisomerase activity (see below), another mode of action. This other mechanism seems to be responsible for the killing of non-dividing bacteria. Based on the results obtained with NAC, it can be speculated that this second mode of action is due to ROS and

oxidative stress generation in bacterial cells. The bactericidal activity against stationary-phase bacteria of organometallic ciprofloxacin derivatives may be useful in the treatment of chronic infectious involving slow-growing or biofilm-forming pathogens.

Topoisomerase inhibitory activity

As mentioned above, quinolones including **CIP** exhibit their major mode of action by suppressing bacterial type IIA topoisomerases, i.e. DNA gyrase and topoisomerase IV.[51, 63] All organometallic ciprofloxacin derivatives except **1** inhibited the introduction of supercoils by *E. coli* gyrase and the decatenation process by *S. aureus* topoisomerase IV at a concentration of 50 μM (Fig. S9). For compounds **3** and **6**, detailed densitometric analyses were performed and the IC_{50} values (concentrations of compounds that inhibit the activity of an enzyme by 50%) were determined (Table 3).

Table 3 IC_{50} values of **3**, **6** and **CIP** for inhibition of *E. coli* DNA gyrase and *S. aureus* topoisomerase IV

	IC_{50} [μM]		
	3	**6**	**CIP**[64]
DNA Gyrase	13.37	2.54	0.15
Topoisomerase IV	6.43	16.85	4.00

The topoisomerases inhibitory activity of both compounds was weaker than that of **CIP**. Compound **6** showed higher inhibitory activity against DNA gyrase (IC_{50} = 2.54 μM) than against topoisomerase IV while compound **3** showed a reverse inhibition pattern. It is well established that among Gram-negative bacteria the primary molecular target for **CIP** is DNA gyrase. In the case of Gram-positive bacteria, topoisomerase IV is the primary molecular target and DNA gyrase plays only a secondary role.[64, 65] In line with this fact, **6** was the most active compound against *E. coli* bacteria and its inhibitory activity of *E. coli* DNA gyrase was much higher than that of topoisomerase IV. On the other hand, the antibacterial activity of **3** was mainly directed against *staphylococci* and its ability to inhibit *S. aureus* topoisomerase IV was stronger than that for DNA gyrase (Table 3, Figure 4).

View Article Online
DOI: 10.1039/C9DT03948A

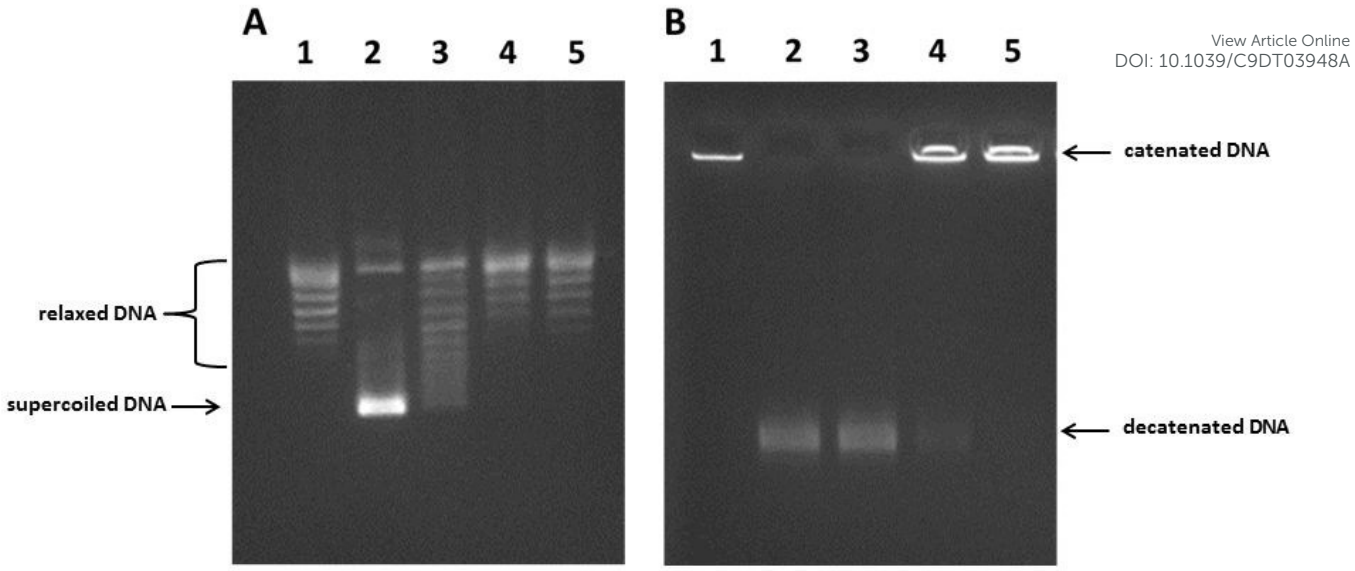

Fig. 4 Inhibition assay for *E. coli* DNA gyrase in the presence of compound **6 (A)** and *S. aureus* topoisomerase IV in the presence of compound **3 (B)**. [**A**: 1 - relaxed pBR – negative control; 2 – *E. coli* DNA gyrase – positive control; 3-5 - compound **6** at concentrations of 5, 10, and 50 μM; **B**: 1 – kinetoplast catenated DNA – negative control; 2 – *S. aureus* topoisomerase IV – positive control; 3-5 – compound **3** at concentration of 5, 10, and 20 μM].

Scanning Electron Microscopy (SEM)

Due to its antibacterial mode of action by inhibiting topoisomerases, **CIP** is known to indirectly affect the expression of many macromolecules within bacterial cell. These changes may manifest in several ways, including disturbances in the production of cell wall components followed by changes in cell shape and size.[66] To determine any structural changes in bacterial morphology upon expose to organometallic ciprofloxacin derivatives, scanning electron microscopic images of the reference *E. coli* and *S. aureus* strains were taken after 12 h treatment with the most promising compounds **4**-**6** and **CIP** (as control) at their MICs. The micrographs showed the smooth morphology of cell surface in non-treated control samples (Fig. 5A and 5F), while the treated cells of both microorganisms displayed roughness or damage to the cell wall or outer membrane. In addition, elongation of *E. coli* cells (Fig. 5B-D) and changes in size and volume of *S. aureus* cells (Fig. 5G-I) were also noticed.

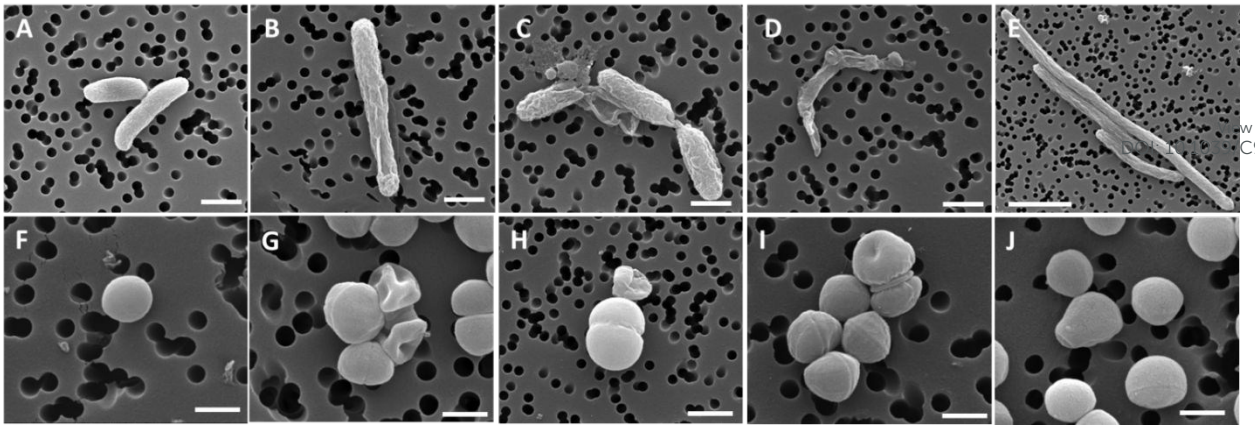

Fig. 5 SEM analysis of bacterial cell morphology after 12 h treatment with derivatives **4**-**6** and **CIP**. Top panels, *E. coli* cells; bottom panels, *S. aureus* cells. (A and F) control, non-treated samples; bacteria treated with compounds 4 (B and G), 5 (C and H), 6 (D and I), and CIP (E and J). Scale bars: 500 nm in F, G, I, and J; 1 μm in A-D and H; 3 μm in E.

Antitrypanosomal activity

The trypanocidal and cytotoxic activity of organometallic ciprofloxacin conjugates **1-6** was evaluated with bloodstream forms of *Trypanosoma brucei* and human acute promyelocytic leukemia HL-60 cells, respectively. Whereas the *N*-acyl conjugated derivatives **1-3** displayed no toxicity towards trypanosomes, the *N*-alkyl conjugated compounds **4-6** showed trypanocidal activity with MIC values of 10 μM and GI_{50} values of around 3 μM (Table 4).

Table 4 MIC (μM) and GI_{50} (μM) values of compounds **1-6** and **CIP** for *T. brucei* bloodstream forms and human HL-60 cells

	T. brucei		HL-60		Selectivity	
Compound	**MIC[a](μM)**	**GI_{50}[b](μM)**	**MIC (μM)**	**GI_{50} (μM)**	**MIC ratio**	**GI_{50} ratio**
1	>100	>100	>100	>100	1	1
2	>100	>100	>100	>100	1	1
3	100	29.2±5.6	>100	>100	>1	>3.4
4	10	3.32±0.32	100	49.3±3.7	10	14.8
5	10	2.83±0.10	100	36.9±0.6	10	13.0
6	10	2.58±0.37	100	35.5±1.8	10	13.8
3	100	29.2±5.6	>100	>100	>1	>3.4
Pp-Cym	>100	62.3±24.7	>100	>100	1	>1.6
CIP	100	30.9±3.3	>100	>100	>1	>3.2
Pp-Cym + CIP	100	30.2±1.8	n.d.	n.d.	n.d.	n.d.
Suramin	0.1-1	0.057±0.005	>100	>100	>100-1000	>1754

[a] MIC (minimum inhibitory concentration, i.e., the concentration of the compound at which all cells were killed); [b] GI_{50} (50% growth inhibition, i.e., the concentration of a compound necessary to reduce the growth rate of cells by 50% to that of controls)

Thus, the toxicity pattern of the compounds against trypanosomes reflects that of the derivatives against bacteria (see above). Encouragingly, compounds **4-6** exhibited more than 10 times less cytotoxicity towards HL-60 cells resulting in moderate selectivity indices (Table 4). In addition, compounds **4-6** were

about 10 times more trypanocidal than unconjugated **CIP**. In order to see whether the trypanocidal activity of the derivatives **4-6** was due to the organometallic component or to a synergistic effect of the organometallic part in combination with **CIP**, we investigated the antitrypanosomal activity of propionyl cymantrene (**Pp-Cym**; Fig. S10) alone and together with **CIP** (Table 4). **Pp-Cym** on its own displayed almost no trypanocidal activity. The combination of **Pp-Cym** and **CIP** exhibited the same trypanocidal activity as **CIP** alone, indicating that there was no synergy between the two compounds. This means that the increased antitrypanosomal activity of derivative **6** was due to the covalent linkage of **Pp-Cym** to **CIP**. For comparison, the trypanocidal activity of suramin, one of the commercial drugs to treat humans infected with *T. brucei*, was also determined. The MIC and GI_{50} values of suramin were 10-100 and 45-58 times lower, respectively, than those of compounds **4-6** (Table 4). As suramin is nontoxic to human HL-60 cells, its selectivity indices were substantially larger. Nevertheless, organometallic *N*-alkyl **CIP** derivatives provide interesting templates for rational antitrypanosomal drug development.

Cytotoxicity

Cytotoxic activity of compounds **1-6** was investigated *in vitro* on non-tumorigenic mouse murine fibroblast L929 and human cervical epithelioid carcinoma HeLa cells using the tetrazolium (MTT) assay. Obtained GI_{50} values are shown in Table 5.

Table 5 Effect of **1-6** and **CIP** on the viability of L929 and HeLa cells after 24 h treatment. The results were expressed as GI_{50} ± SEM from three independent experiments (n = 3)

	GI_{50} [μM]						
	1	**2**	**3**	**4**	**5**	**6**	**CIP**
L929	61±2.7	33±1.0	85±2.2	111±5.4	58±4.9	87±8.7	>1000±nd
HeLa	63±3.1	71±4.6	27±1.3	97±10.7	36±3.5	58±4.6	560±22.6

nd – not determined

All **CIP** conjugates, including the three most active derivatives against bacteria (**3**, **5**, and **6**) were also found to be toxic for cell lines. Human HeLa cells were more sensitive to the compounds than murine fibroblasts. All derivatives decreased cell viability more than **CIP**. However, the GI_{50} values were significantly higher than the corresponding MIC values. To visualize this, GI_{50}/MIC ratios were calculated as a parameter demonstrating the selectivity of **1-6** towards bacterial cells (Table 6).

Table 6 Selectivity of compound **1-6** towards bacterial cells expressed as GI_{50}/MIC ratios where GI_{50}, the concentration that inhibited mammalian cells viability by 50%, is divided by the bacterial MIC value.

View Article Online
DOI: 10.1039/C9DT03948A

	GI_{50}/MIC [Range]					
	1	**2**	**3**	**4**	**5**	**6**
L929	2-10	1-3	$3\text{-}11\text{x}10^{1}$	$18\text{-}14\text{x}10^{2}$	$19\text{-}96\text{x}10^{3}$	$93\text{-}29\text{x}10^{5}$
HeLa	3-10	3-6	1-34	$16\text{-}12\text{x}10^{1}$	$12\text{-}60\text{x}10^{3}$	$19\text{-}58\text{x}10^{5}$

Thus, a larger ratio (i.e. bigger difference between GI_{50} and MIC values) for a particular compound means a lesser risk of its toxic side-effects when used as an antibacterial agent. The effective antibacterial concentrations of compounds **5** and **6** were found to be more than $10^3 – 10^5$ times lower than their toxic concentrations for L929 and HeLa cells.

View Article Online
DOI: 10.1039/C9DT03948A

Conclusions

This study has shown that the linkage of the antibiotic ciprofloxacin with organometallic moieties yielded conjugates with potent antimicrobial activity. Several conjugates displayed increased bactericidal and bacteriostatic activity against Gram-negative and Gram-positive bacteria as well as against MRSA strains. In addition, some derivatives showed improved antitrypanosomal activity when compared to their unconjugated starting compounds. The most potent derivatives were *N*-alkyl cymantrenyl and ruthenocenyl conjugates of ciprofloxacin. The observed increased antimicrobial activity of the conjugates was most likely due to two mechanisms of action; inhibition of DNA gyrase and topoisomerase IV by ciprofloxacin moiety and ROS production by the organometallic moiety. In conclusion, this study has demonstrated that the conjugation of organometallics to antimicrobial drugs is a promising approach in the search for new antibiotics. In addition, antimicrobial agents with dual or multiple modes of action may be a promising strategy in combating drug resistance.

Experimental

General methods

All preparations were carried out using standard Schlenk techniques. Chromatographic separations used silica gel 60 (Merck, 230-400 mesh ASTM). DMF was distilled and purged with argon prior to use. Other solvents were of reagent grade and used without prior purification. Ciprofloxacin and carboxylic acids **A-C** were purchased from commercial supplier and used without further purification. Compounds D-F were obtained according to literature.[53,54] ^{1}H NMR (600 MHz) and ^{13}C{H} NMR (150 MHz) spectra were recorded on a Bruker Avance III 600 spectrometer operating at 298 K. Chemical shifts are reported in δ units (ppm) using the residual signal of DMSO (^{1}H δ 2.50 ppm, ^{13}C δ 39.70) as reference. EI mass spectra were recorded on a Finnigan MAT 95 mass spectrometer. Electrospray mass spectra were obtained on a ThermoFisher Exactive Plus instrument with an Orbitrap mass analyser in positive ion mode at a resolution of R = 70.000 and a solvent flow rate of 10 μL min^{-1} using acetonitrile as solvent. For protein interaction study, water was used as solvent and the flow rate was increased to 100 μL min^{-1}. Only the most prominent peak of each isotope pattern is reported. IR spectra (KBr pellets) were measured on a FTIR Nexus Nicolet apparatus. Microanalyses were carried out by the Analytical Services of the Polish Academy of the Sciences (Łódź).

Synthesis

General procedure for the synthesis of compounds **1-3**

Ciprofloxacin **A** (116 mg, 0.35 mmol), 1-ethyl-3-(3-dimethylaminopropyl)carbodiimide hydrochloride (75 mg, 0.39 mmol) and 4-(dimethylamino)pyridine (4.3 mg, 0.04 mmol) were subsequently added to a stirred solution of either ferrocene carboxylic acid **A** (81 mg, 0.35 mmol), ruthenocene carboxylic acid **B** (96 mg, 0.35 mmol), or cymantrene carboxylic acid **C** (87 mg, 0.35 mmol) in dichloromethane (20 mL) at 0 °C. The reaction mixture was stirred at ambient temperature for 24 h. Then, the reaction mixture was poured onto water, washed once with 5 mL of 5% HCl_{aq} and extracted with dichloromethane. The organic layer was separated, dried over anhydrous $MgSO_4$, filtered and all volatiles were evaporated under reduced pressure. The remaining material was subjected to column chromatography on silica gel with dichloromethane/methanol (50:1 v/v) as eluent. Crystallization from a dichloromethane/*n*-hexane mixture gave analytically pure samples. Compound **1** was obtained as a yellow solid (153 mg, 80% yield), **2** as a colorless solid (105 mg, 51% yield) and **3** as a beige solid (102 mg, 52% yield), respectively.

1: ^{1}H NMR (600 MHz, DMSO-d_6): δ = 15.19 (s, 1H, COOH), 8.67 (s, 1H, =C-H), 7.94 (d, J_{HF} = 12.6 Hz, 1H, H_{arom}), 7.61 (bs, 1H, H_{arom}), 4.62 (s, 2H, α-C_5H_4), 4.42 (s, 2H, β-C_5H_4), 4.28 (s, 5H, C_5H_5), 3.92 (bs, 4H, $C_4H_8N_2$), 3.82 (s, 1H, CH cyclopropyl), 3.41 (s, 4H, $C_4H_8N_2$), 1.33 (s, 2H, CH_2 cyclopropyl), 1.19 (s, 2H, CH_2 cyclopropyl). EI-MS: *m*/*z* = 566 $[M+Na]^+$, 544 $[M+H]^+$. FTIR (KBr ν [cm^{-1}]): 3431 (COOH), 3110, 3082, 3055, 2862, 1743 (C=O), 1614 (C=O), 1509, 1493, 1468, 1455, 1256, 1029, 1009, 828. Anal. Calcd for $C_{28}H_{26}N_3O_4FFe$ (%): C 61.89, H 4.82, N 7.73; Found: C 61.74, H 4.78, N 7.75.

2: ^{1}H NMR (600 MHz, DMSO-d_6): δ = 15.19 (s, 1H, COOH), 8.67 (s, 1H, =C-H), 7.94 (d, J_{HF} = 13.2 Hz, 1H, H_{arom}), 7.60 (d, J_{HF} = 7.2 Hz, 1H, H_{arom}), 4.92 (pt, J_{HH} = 1.8 Hz, 2H, α-C_5H_4), 4.75 (s, J_{HH} = 1.8 Hz, 2H, β-C_5H_4), 4.70 (s, 5H, C_5H_5), 3.89 (bs, 4H, $C_4H_8N_2$), 3.82 (s, 1H, CH cyclopropyl), 3.36 (s, 4H, $C_4H_8N_2$), 1.33 (m, 2H, CH_2 cyclopropyl), 1.19 (m, 2H, CH_2 cyclopropyl). EI-MS: *m*/*z* = 590 $[M+H]^+$. FTIR (KBr ν [cm^{-1}]): 3399 (COOH), 3111, 3058, 2960, 2886, 2859, 1743 (C=O), 1616 (C=O), 1510, 1498, 1467, 1441, 1254, 1025, 1008, 822. Anal. Calcd for $C_{28}H_{26}N_3O_4FRu$ (%): C 57.14, H 4.45, N 7.14; Found: C 57.23, H 4.38, N 6.89.

3: ^{1}H NMR (600 MHz, DMSO-d_6): δ = 15.16 (s, 1H, COOH), 8.67 (s, 1H, =C-H), 7.94 (d, J_{HF} = 12.6 Hz, 1H, H_{arom}), 7.58 (bs, 1H, H_{arom}), 5.58 (s, 2H, α-C_5H_4), 5.09 (s, 2H, β- C_5H_4), 3.79 (bs, 5H, $C_4H_8N_2$ + CH cyclopropyl), 3.38 (bs, 4H, $C_4H_8N_2$), 1.32 (s, 2H, CH_2 cyclopropyl), 1.18 (s, 2H, CH_2 cyclopropyl). $^{13}C\{^1H\}$ NMR (150 MHz, DMF-d_7): δ = 225.1,

177.3, 166.5, 163.6, 156.9 (d,$^{1}J_{CF}$ = 249.0 Hz), 148.5, 145.6 (d, $^{2}J_{CF}$ = 10.3 Hz), 139.9, 119.8, 111.4 (d, $^{2}J_{CF}$ = 23.1 Hz), 107.6, 107.2, 97.0, 87.9, 83.0, 50.1, 47.0, 36.3, 7.9. ES-MS: *m*/*z* = 562 $[M+H]^{+}$. FTIR (KBr ν [cm^{-1}]): 3055, 2913, 2865, 2022 (Mn-CO), 1970 (Mn-CO), 1917 (Mn-CO), 1724 (C=O), 1627 (C=O), 1506, 1472, 1455, 1422, 1256, 1182, 1011. Anal. Calcd for $C_{26}H_{21}N_3O_7FMn$ (%): C 55.63, H 3.77, N 7.48; Found: C 55.59, H 3.77, N 7.44.

General procedure for the synthesis of compounds **4**-**6**

Triethylamine (97 μL, 0.7 mmol) was added to a stirred solution of either (3-chloropropionyl)-ferrocene **D** (97 mg, 0.35 mmol), (3-chloropropionyl)-ruthenocene **E** (113 mg, 0.35 mmol), or (3-chloropropionyl)-cymantrene **F** (103 mg, 0.35 mmol) in *N*,*N*-dimethylformamide (15 mL) at ambient temperature. After 20 min of stirring, ciprofloxacin (116 mg, 0.35 mmol) was added, and the reaction mixture was stirred at a temperature of either 85 °C for 5 h in case of **D** and **E** or 75 °C for 4 h in case of **F**. Subsequently, all volatiles were evaporated under reduced pressure and the residue was dissolved in dichloromethane (~10 mL), washed with 5 mL of 5% HCl_{aq} and extracted with dichloromethane. The organic layer was dried over $MgSO_4$, filtered and evaporated to dryness. The residue was subjected to column chromatography on silica gel with dichloromethane/methanol (50:1 v/v) as eluent. Crystallization from a dichloromethane/*n*-hexane mixture gave analytically pure samples. Compound **4** was obtained as an orange solid (160 mg, 80% yield), **5** as a yellow solid (188 mg, 87% yield) and **6** as a pale orange solid (175 mg, 85% yield).

4: ^{1}H NMR (600 MHz, DMSO-d_6): δ = 15.20 (s, 1H, COOH), 8.65 (s, 1H, =C-H), 7.90 (d, J_{HF} = 12.6 Hz, 1H, H_{arom}), 7.56 (bs, 1H, H_{arom}), 4.84 (s, 2H, α-C_5H_4), 4.58 (s, 2H, β-C_5H_4), 4.27 (s, 5H, C_5H_5), 3.83 (s, 1H, CH cyclopropyl), 3.34 (s, 4H, $C_4H_8N_2$), 2.95 (bs, 2H, CH_2), 2.76 (bs, 2H, CH_2), 2.68 (s, 4H, $C_4H_8N_2$), 1.30 (s, 2H, CH_2 cyclopropyl), 1.18 (s, 2H, CH_2 cyclopropyl). $^{13}C\{^{1}H\}$ NMR (150 MHz, DMSO-d_6): δ =202.4, 176.4, 166.0, 164.0, 153.1 (d,$^{1}J_{CF}$ = 249.9 Hz), 148.1, 145.3 (d, $^{2}J_{CF}$ = 10.3 Hz), 139.3, 118.6, 111.0 (d, $^{2}J_{CF}$ = 23.1 Hz), 106.8, 106.4, 79.3, 72.3, 69.7, 69.3, 52.9, 52.6, 49.6, 36.6, 7.7. EI-MS: *m*/*z* = 572 $[M+H]^{+}$. FTIR (KBr ν [cm^{-1}]): 3420 (COOH), 3088, 2952, 2930, 2875, 1724 (C=O), 1663 (C=O), 1628 (C=O), 1612 (C=O), 1506, 1494, 1458, 1380, 1338, 1260. Anal. Calcd for $C_{30}H_{30}N_3O_4FFe$ (%): C 63.06, H 5.29, N 7.35; Found: C 63.06, H 5.56, N 7.28.

5: ^{1}H NMR (600 MHz, DMSO-d_6): δ = 15.20 (s, 1H, COOH), 8.66 (s, 1H, = C-H), 7.90 (d, J_{HF} = 13.2 Hz, 1H, H_{arom}), 7.56 (d, J_{HF} = 7.8 Hz, 1H, H_{arom}), 5.15 (pt, J_{HH} = 1.8 Hz, 2H, α-C_5H_4), 4.85 (pt, J_{HH} = 1.8 Hz, 2H, β-C_5H_4), 4.65 (s, 5H, C_5H_5), 3.82 (m, 1H, CH cyclopropyl),

3.33 (t, J_{HH} = 4.2 Hz, 4H, $C_4H_8N_2$), 2.81 (t, J_{HH} = 7.2 Hz, 2H, CH_2), 2.69 (t, J_{HH} = 7.2 Hz, 2H, CH_2), 2.63 (t, J_{HH} = 4.2 Hz, 4H, $C_4H_8N_2$), 1.30 (pq, J_{HH} = 6.0 Hz, 2H, CH_2 cyclopropyl), 1.18 (pt, J_{HH} = 6.0 Hz, 2H, CH_2 cyclopropyl). $^{13}C\{^1H\}$ NMR (150 MHz, DMSO-d_6): δ = 200.4, 176.4, 166.0, 153.1 (d, $^1J_{CF}$ = 249.6 Hz), 148.1, 145.3 (d, $^2J_{CF}$ = 10.3 Hz), 139.3, 118.6, 111.0 (d, $^2J_{CF}$ = 23.1 Hz), 106.8, 106.4, 84.0, 73.7, 72.0, 70.7, 55.0, 53.3, 52.4, 49.5, 36.0, 7.7. EI-MS: m/z = 618 $[M+H]^+$. FTIR (KBr ν [cm^{-1}]): 3446 (COOH), 3091, 2908, 2838, 1730 (C=O), 1672 (C=O), 1629 (C=O), 1612 (C=O), 1502, 1463, 1260. Anal. Calcd for $C_{30}H_{30}N_3O_4FRu$ (%): C 58.43, H 4.90, N 6.81; Found: C 58.29, H 4.82, N 6.70.

6: ^1H NMR (600 MHz, DMSO-d_6): δ = 15.20 (s, 1H, COOH), 8.65 (s, 1H, =C-H), 7.90 (d, J_{HF} = 13.8 Hz, 1H, H_{arom}), 7.55 (d, J_{HF} = 6.0 Hz, 1H, H_{arom}), 5.85 (s, 2H, α-C_5H_4), 5.22 (s, 2H, β-C_5H_4), 3.83 (s, 1H, CH cyclopropyl), 3.30 (4H of the $C_4H_8N_2$ moiety are under the residual water signal), 2.87 (t, J_{HH} = 7.2 Hz, 2H, CH_2), 2.71 (t, J_{HH} = 7.2 Hz, 2H, CH_2), 2.64 (s, 4H, $C_4H_8N_2$), 1.30 (d, J_{HH} = 5.4 Hz, 2H, CH_2 cyclopropyl), 1.18 (s, 2H, CH_2 cyclopropyl). $^{13}C\{^1H\}$ NMR (150 MHz, DMSO-d_6): δ = 223.8, 196.7, 176.5, 166.1, 156.5, 153.1 (d, $^1J_{CF}$ = 252.0 Hz), 148.0, 145.2 (d, $^2J_{CF}$ = 10.3 Hz), 139.2, 118.6, 111.0 (d, $^2J_{CF}$ = 23.1 Hz), 106.7, 106.3, 92.2, 87.7, 85.2, 52.4, 52.3, 49.4, 36.2, 7.6. EI-MS: m/z = 590 $[M+2H]^+$. FTIR (KBr ν [cm^{-1}]): 3433 (COOH), 3065, 2951, 2905, 2845, 2020 (Mn-CO), 1925 (Mn-CO), 1725 (C=O), 1675 (C=O), 1629 (C=O), 1497, 1467. Anal. Calcd for $C_{28}H_{25}N_3O_7FMn$ (%): C 57.05, H 4.27, N 7.13; Found: C 57.01, H 4.48, N 6.91.

X-ray structure analysis

Good quality single-crystals of **4** and **6** were selected for X-ray diffraction experiments at T = 100(2) K. Diffraction data were collected on an Agilent Technologies SuperNova Dual Source diffractometer with Cu$K\alpha$ radiation (λ = 1.54184 Å) using CrysAlis RED software.[67] The analytical numerical absorption correction using a multifaceted crystal model based on expressions derived by R.C. Clark & J.S. Reid[68] implemented in SCALE3 ABSPACK scaling algorithm was applied for both compounds.[67] The structural determination procedure was carried out using the SHELX package.[69] The structures were solved with direct methods and then successive least-square refinement was carried out based on the full-matrix least-squares method on F^2 using the SHELXL program.[69] The H-atoms linked to O-atoms were located from the Fourier difference electron density map and refined with $U_{iso}(H) = 1.5U_{eq}(O)$. Remaining H-atoms were positioned geometrically, with C–H equal to 0.93, 0.97 and 0.98 Å for the aromatic, methylene and methine H-atoms, respectively, and constrained to ride on

View Article Online
DOI: 10.1039/C9DT03948A

their parent atoms with $U_{iso}(H) = 1.2U_{eq}(C)$. In case of **6**, a few distinct peaks on the difference Fourier map indicated the presence of a disordered solvent molecule. All attempts to model a disordered solvent used for crystallization failed. Therefore, the solvent contribution has been removed applying the appropriate MASK procedure in Olex2 program.[70] Calculated solvent accessible volume was approximately 174.9 Å^3 occupied by 52.6 electrons per unit cell. The cyclopropyl fragment in **6** was disordered over two positions with refined occupancy ratio of 0.62(2) : 0.38(2). All C−C bond lengths of disordered moiety were subject of SADI restraints. In case of the ferrocenyl **4**, RIGU restraint was applied. All molecular interactions in the crystals were identified using PLATON program.[71] The figures for this publication were prepared using Olex2 and Mercury programs.[70,72]

The CCDC 1952897 (**4**) and 1952898 (**6**) contains the supplementary crystallographic data for this paper. The data can be obtained free of charge from the Cambridge Crystallographic Data Center via www.ccdc.cam.ac.uk/structures.

Methods

Biology

Antibacterial activity evaluation

The *in vitro* antimicrobial activity of the six organometallic ciprofloxacin derivatives was evaluated using a set of reference Gram-negative bacteria strains (*E. coli* ATCC 25922, *E. coli* NCTC 8196, *P. vulgaris* ATCC 49990, *K. pneumoniae* ATCC 13883*)* and Gram-positive bacteria strains (*S. aureus* ATCC 6538, *S. aureus* ATCC 29213, *S. epidermidis* ATCC 12228). In addition, two clinical isolates of methicillin-resistant *S. aureus* (MRSA) obtained from infected bones of patients hospitalized at the Oncological Hospital in Łódź (Poland), as well as a *S. aureus* ATCC 6538 mutant resistant to high concentrations of ciprofloxacin were also tested. All strains were kept frozen at −80 °C on Tryptic Soy Broth with 15% of glycerol until testing. The minimal inhibitory concentration (MIC) was defined as the lowest concentration of the compound preventing visible growth of the microorganism using the microdilution method according to EUCAST guidelines [ISO 20776-1 (2006)]. Each compound was pipetted into wells of 96-well microplates as a series of two-fold dilutions in Mueller-Hinton broth in the concentration range from 0.2 to 50 μM. For the most active compounds, further dilutions were made in order to determine their MIC values. All compounds were dissolved in dimethylformamide (DMF)[73] The final concentration of DMF in media was 1% which had no influence on the growth of the microorganisms. Then, bacteria were added at an inoculum of approximately 5×10^5 CFU/mL. The plates were incubated at

37°C for 18 h and the optical density (OD_{600}) was measured using SpectraMax i3 Multi-Mode Platform (Molecular Devices).

Minimal bactericidal concentration (MBC), defined as the lowest concentration of a compound that resulted in >99.9% reduction in CFU/mL of the initial inoculum, was determined following MIC evaluation by plating out the contents of the first well that showed no visible growth of bacteria, as well as the two next wells with higher concentrations of the compound onto Mueller-Hinton agar plates. Then, the plates were incubated at 37 °C for 18 h. Ciprofloxacin hydrochloride (CIP, Sigma-Aldrich PHR-1044) was used as a reference antimicrobial agent for both MIC and MBC measurements. All evaluations were performed in triplicates.

Selection of *S. aureus* CIP^R

Staphylococcus aureus ATCC 6538 mutant resistant to high concentrations of ciprofloxacin (CIP^R) was obtained in our laboratory through selection on agar plates with increasing concentrations of the antibiotic. Initially, an inoculum of 2 x 10^8 CFU/mL of the wild type *S. aureus* ATCC 6538 was plated on agar plates containing ciprofloxacin at the concentration of ¼ MIC. After 24 h incubation, growing colonies were transferred to plates containing increasingly higher concentrations of ciprofloxacin of 1/2 MIC, MIC, 2 x MIC, 4 x MIC, etc., until the resulting mutants were resistant to 60 x MIC of CIP. The selected individual colonies of the obtained mutant were then transferred to the Mueller-Hinton broth medium supplemented with 10 x MIC of ciprofloxacin, incubated overnight and used for susceptibility testing. Several passages were performed in order to check the stability of phenotype.

Antibacterial activity in the presence of NAC

The antibacterial activity of compounds in the presence of the antioxidant *N*-acetyl-L-cysteine (NAC) was determined in the same way as described above, except that 5 µL of NAC was added to each well to give a final concentration of 10 mM/well. In addition, the influence of NAC itself on bacterial growth was also assessed. All evaluations were performed in triplicates.

Antibacterial studies of stationary-phase *E. coli* and *S. aureus*

High cell density stationary-phase cultures of *E. coli* ATCC 25922 and *S. aureus* ATCC 29213 grown in Mueller-Hinton broth for 24 h were treated with 0.1 µM of **4**, **5**, **6** and 2 µM of **3**, **6**, respectively. After 24 h incubation, the number of CFU/mL was determined by seeding serial dilutions of cultures on agar plates. Ciprofloxacin hydrochloride was used as a control antimicrobial agent. The results were presented as mean CFU/mL ± SEM from three

independent experiments. Comparisons between tested compounds and untreated control were made using One-way ANOVA analysis of variance with Tukey's multiple comparison post-test.

Topoisomerases inhibition

The inhibitory activity of the six organometallic ciprofloxacin derivatives against *E. coli* DNA gyrase and *S. aureus* topoisomerase IV was evaluated using a gyrase supercoiling assay kit and a topoisomerase IV decatenation kit (Inspiralis, K0001 and SAD4001). The supercoiling assay was performed using a relaxed pBR322 plasmid (0.5 μg) as a substrate. The DNA was incubated with 1 U of gyrase in the provided supercoiling assay buffer in the presence of 50 μM of test compounds. Reactions were carried out at 37 °C for 1 h and then terminated by the addition of an equal volume of 2 × STOP Buffer (40% sucrose, 100 mM Tris-Cl pH 7.5, 1 mM EDTA, and 0.5 mg/mL bromophenol blue) and chloroform/isoamyl alcohol. Samples were vortexed, centrifuged and separated on a 0.8 % agarose gel in TAE buffer (40 mM Tris-acetate, 2 mM EDTA) for 2 h at 70 V. After electrophoresis, gels were stained with ethidium bromide and visualized under UV light. The decatenation assay was performed using an interlinked kDNA substrate (0.5 μg) incubated with 1 U of topoisomerase IV in the provided decatenation assay buffer in the presence of 50 μM of the test compounds. Reactions were carried out at 37 °C and electrophoresis was performed under same conditions as described for the supercoiling assay. For two selected compounds (**3** and **6**), detailed analyzes were performed by using a concentration range of 5-50 μM. IC_{50} values (concentration that inhibited the activity of the enzymes by 50%) were determined based on densitometric evaluations of electrophoregrams using Quantity One software (BioRad).

Scanning Electron Microscopy

To evaluate the effect of the compounds **4-6**, as well as **CIP** on bacterial cells, their morphology was studied by SEM as previously described.[74] Briefly, compounds were added to bacterial cell cultures at a concentration equal to their MIC values and incubated for 12 h under shaking (37 ºC). Then, bacterial samples were washed with PBS (0.1 M), fixed in glutaraldehyde (2.5%) for 90 min, and dehydrated in ethanol solutions (30-100%) twice for 15 min. Prior to SEM visualization, samples were coated with Pt (15 nm). SEM images were acquired using SEM Inspect F50 (10-15keV; FEI Co., LMA-INA, Spain).

Antitrypanoosmal activity evaluation

The trypanocidal activity of organometallic ciprofloxacin derivatives was determined with bloodstream forms of *T. brucei* 427/221[75] using the resazurin vital dye method.[76] For comparison, compounds were also tested for their cytotoxic effect on human leukemia HL-60

View Article Online
DOI: 10.1039/C9DT03948A

cells. Cells were seeded in 96-well plates in a final volume of 200 µl of Baltz medium[77] supplemented with 16.7% bovine serum containing different concentrations of test compounds (10^{-4} to 10^{-9} M) and 0.9% DMSO. Wells containing medium and 0.9% DMSO served as controls. The initial densities were 1×10^4/ml trypanosomes and 5×10^4/ml HL-60 cells. After 24 h incubation at 37 °C in a humidified atmosphere containing 5% CO_2, 20 µl of a 0.5 mM resazurin solution prepared in sterile PBS was added and the cells were incubated for a further 48 h so that the total incubation time was 72 h. Then, the plates were read on a microplate reader using a test wavelength of 570 nm and a reference wavelength of 630 nm. GI_{50} values were calculated by linear interpolation using the method of Huber and Koella.[78] MIC values were determined microscopically.

Cell viability assay

The effect of the six organometallic ciprofloxacin derivatives on the viability of mammalian cells was determined with the MTT reduction assay. Murine fibroblasts L929 cells (ATTC ®—CCL-1) and human tumor HeLa cells (ATTC ®—CCL-2™) were plated in 96-well microplates at a density of 1×10^4 cells/well according to international standard ISO 10993-5:2009(E) (American National Standard 2009) in Dulbecco's Modified Eagle Medium (DMEM, Biowest) supplemented with 10% fetal bovine serum (FBS, Biowest), 100 U/mL of penicillin, and 100 µg/mL of streptomycin (Biowest). Cell cultures were incubated at 37 °C in a humidified atmosphere containing 5% CO_2. After overnight incubation, growth medium was removed and 100 µL of fresh medium supplemented with two-fold dilutions of test compounds in a concentration range of 0.4–50 µM were added. All test compounds were dissolved in DMF, which final concentration in medium did not exceed 1%. Thus, DMF at the concentration of 1%, served as a negative control, however, concentrations of DMF up to 2% were found not harmful to the tested cell lines (data not shown). After 24 h incubation, the medium was removed and 3-(4,5-dimethylthiazol-2-yl)-2,5-diphenyltetrazolium bromide (MTT, Sigma-Aldrich M-5655) at a concentration of 50 µg/well was added. Plates were incubated for the next 2 h at 37 °C, 5% CO_2. Then, formazan crystals were solubilized in 150 µL DMSO and quantified by spectrophotometric measurement at 550 nm by using SpectraMax i3 Multi-Mode Platform (Molecular Devices). The results of the experiments were shown as mean arithmetic values from 3 repeats in each of two independent experiments and the percentage of viability inhibition was calculated in comparison with the untreated controls. GI_{50} values (drug concentration that inhibits cell viability by 50%) were calculated with the Prism GraphPad 7 software using nonlinear regression. Additionally, the GI_{50}/MIC

ratio was determined for each of the compounds in order to evaluate their selective activity towards bacteria in comparison to mammalian cells.

Conflicts of interest

There are no conflicts of interest to declare

ACKNOWLEDGMENTS

Crystallographic measurements were carried out at the Biological and Chemical Research Centre, University of Warsaw, established within the project co-financed by European Union from the European Regional Development Fund under the Operational Programme Innovative Economy, 2007 – 2013. The X-ray diffraction data collection was accomplished at the Core Facility for Crystallographic and Biophysical Research to support the development of medicinal products sponsored by the Foundation for Polish Science (FNP).

References

1. B. Albada and N. Metzler-Nolte, *Chem. Rev.*, 2016, **116**, 11797-11839.

2. G. Gasser, I. Ott and N. Metzler-Nolte, *J. Med. Chem.*, 2011, **54**, 3-25.

3. K. Kowalski, *Coord. Chem. Rev.*, 2018, **366**, 91-108.

4. Y. C. Ong, S. Roy, P. C. Andrews and G. Gasser, *Chem. Rev.*, 2019, **119**, 730-796.

5. J, -L. H, A, Duprey and J. H. R Tucker, *Chem. Lett.*, 2014, **43**, 157-163.

6. M. Pataya and G. Gasser, *Nat. Rev. Chem.*, 2017, **1**, 0066.

7. I. R. Krauss, G. Ferraro, A. Pica, J. A. Márquez, J. R. Helliwell and A. Merlino, *Metallomics,* 2017, **9**, 1534-1547.

8. I. Ott, B. Kircher, C. P. Bagowski, D. H. W. Vlecken, E. B. Ott, J. Will, K. Bensdorf, W. S. Sheldrick and R. Gust, *Angew. Chem., Int. Ed.*, 2009, **48**, 1160-1163.

9. S. Thora, D. A. Rodrigues, D. C. Crans and E. J. Barreiro, *J. Med. Chem.*, 2018, **61**, 5805-5821.

10. L. E. Jennings and N. J. Long, *Chem. Commun.*, 2009, 3511-3524

11. G. Jaouen, A. Vessières and S. Top, *Chem. Soc. Rev.*, 2015, **44**, 8802-8817.

12. K. M. G. O'Connell, J. T. Hodgkinson, H. F. Sore, M. Welch, G. P. C Salmond and D. R. Spring, *Angew. Chem., Int. Ed.*, 2013, **52**, 10706-10733.

13. S. B. Levy and B. Marshall, *Nat. Med.*, 2004, **10**, S122-S129.

14. A. S. Nagle, S. Khare, A. B. Kumar, F. Supek, A. Buchynskyy, C. J. N. Mathison, N. K. Chennamaneni, N. Pendem, F. S. Buckner, M. H. Gelb and V. Molteni, *Chem. Rev.*, 2014, **114**, 11305-11347.

15. R. A. Sanchez-Delgado, A. Anzellotti, and L. Suarez, *Met. Ions Biol. Syst.*, 2004, **41**, 379-419.

16. A. Mederos, Z. Ramos and G. Banchero, *Parasites&Vectors*, 2014, **7**, 598-601.

17. M. A. Sierra, L. Casarrubios and M. C. de la Torre, *Chem. Eur. J.*, 2019, 25, 7232-7242.

18. M. Patra, G. Gasser and N. Metzler-Nolte, *Dalton Trans.*, 2012, **41**, 6350-6358.

19. E. I. Edwards, R. Epton and G. Marr, *J. Organomet. Chem.*, 1975, **85**, C23-C25.

20. J. Skiba, A. Rajnisz, K. N. de Oliveira, I. Ott, J. Solecka and K. Kowalski, *Eur. J. Med. Chem.*, 2012, **57**, 234-239.

21. E. M. Lewandowski, J. Skiba, N. J. Torelli, A. Rajnisz, J. Solecka and K. Kowalski, *Chem. Commun.*, 2015, **51**, 6186-6189.

22. E. M. Lewandowski, Ł. Szczupak, S. Wong, J. Skiba, A. Guśpiel, J. Solecka, V. Vrček, K. Kowalski and Y. Chen, *Organometallics*, 2017, **36**, 1673-1676.

23. E. M. Lewandowski, K. G. Lethbridge, R. Sanishvili, J. Skiba, K. Kowalski and Y. Chen, *The FEBS* Journal, 2018, **285**, 87-100.

24. M. Mbaba, A. N. Mabhula, N. Boel, A. L. Edkins, M. Isaacs, H. C. Hoppe and S. D. Khanye, *J. Inorg. Biochem.*, 2017, **172**, 88-93.

25. M. Patra. G. Gasser, M. Wenzel, K. Merz, J. E. Bandow and N. Metzler-Nolte, *Organometallics*, 2010, **29**, 4312-4319.

26. M. Patra. G. Gasser, M. Wenzel, K. Merz, J. E. Bandow and N. Metzler-Nolte, *Organometallics*, 2012, **31**, 5760-5771.

27. C. Biot and D. Dive, Bioorganometallic Chemistry and Malaria. In: *Topics in Organometallic Chemistry*, ed. N. Metzler-Nolte, G. Jaouen, Springer: Berlin, 2010; **32**, 155-194

28. M. Navarro, W. Castro and C. Biot, *Organometallics*, 2012, **31**, 5715-5727.

29. P. V. Simpson, C. Nagel, H. Bruhn and U. Schatzschneider, *Organometallics*, 2015, **34**, 3809-3815.

30. F. Dubar, G. Anquetin, B. Pradines, D. Dive, J. Khalife and C. Biot, *J. Med. Chem.*, 2009, **52**, 7954-7957.

31. L. Glans, W. Hu, C. Jöst, C. de Kock, P. J. Smith, M. Haukka, H. Bruhn, U. Schatzschneider and E. Nordlander, *Dalton. Trans.*, 2012, **41**, 6443-6450.

32. M. Patra, K. Ingram, A. Leonidova, V. Pierroz, S. Ferrari, M. N. Robertson, M. H. Todd and G. Gasser, *J. Med. Chem.*, 2013, **56**, 9192-9198.

33. J. Hess, M. Patra, V. Pierroz, B. Spingler, A. Jabbar, S. Ferrari, R. B. Gasser and G. Gasser, *Organometallics*, 2016, **35**, 3369-3377.

34. G. Y. Lesher, E. J., Froelich, M. D. Gruett, J. H. Bailey and R. P. Brundage, *J. Med. Pharm. Chem*., 1962, **91**, 1063-1065.

35. H. Koga, A. Itoh, S. Murayama, S. Suzue and T. Irikura, *J. Med. Chem.*, 1980, **23**, 1358-1363.

36. I. Hayakawa, T. Hiramitsu and Y. Tanaka, *Chem. Pharm. Bull.*, 1984, **34**, 4907-4913.

37. K. Grohe and H. Heitzer, *Liebigs Ann. Chem.*, 1987, **1**, 29-37.

38. D. L. Anderson, *Drugs Today,* 2008, **44**, 489-501.

39. M. R. Jacobs and P. C. Appelbaum, *Expert Opin. Pharmacother.*, 2006, **7**, 1957-1966.

40. R.J. Anderson, P.W. Groundwater, A. Todd, A.J. Worsley, in *Antibacterial Agents:Chemistry, Mode of Action, Mechanisms of Resistance and Clinical Applications*, John Wiley & Sons, Inc., 2012

41. L. A. Mitscher, *Chem. Rev.*, 2005, **105**, 559-592.

42. D. J. Dwyer, M. Kohanski, B. Hayete and J. J. Collins, *Mol. Syst. Biol.*, 2007, **3**, 91.

43. J. J. Foti, B. Devadoss, J. A. Winkler, J. J. Collins and G. C. Walker, *Science*, 2012, **336**, 315-319.

44. P. F. Chan, J. Huang, B. D. Bax and M. N. Gwynn, Recent developments in inhibitors of bacterial type IIA topoisomerases. in: *Antibiotics: Targets, Mechanisms and Resistance*, ed. C. O. Gualerzi, L. Brandi, A. Fabbretti and C. L Pon, Wiley, Weinheim, 2013, 263-297.

45. N. G. Bush, K. Evans-Roberts and A. Maxwell, *Ecosal. Plus*, 2015, **6**, 1-34.

46. A. J. Schoeffler and J. M. Berger, *Q. Rev. Biophys.*, 2008, **41**, 41-101.

47. M. Nöllmann, N. J. Crisona, P. B. Arimondo, *Biochimie*, 2007, **89**, 490-499.

48. V. Srikannathasan, A. Wohlkonig, A. Shillings, O. Singh, P. F. Chan, J. Huang, M. N. Gwynn, A. P. Fosberry, P. Homes, M. Hibbs, A. J. Theobald, C. Spitzfaden and B. D. Bax, *Acta Crystallogr., Sect. F: Struct. Biol. Commun.,* 2015, **71**, 1242-1246.

49. T. R. Blower, B. H. Williamson, R. J. Kerns and J. M. Berger, *Proc. Nat. Acad. Sci. USA*, 2016, **113**, 1706-1713.

50. K. J. Aldred, R. J. Kerns and N. Osheroff, *Biochemistry*, 2014, **53**, 1565-1574.

51. L. S. Redgrave, S. B. Sutton, M. A. Webber and L. J. V. Piddock, *Trends Microbiol.*, 2014, **22**, 438-445.

52. S. Kalghatgi, C. S. Spina, J. C. Costello, M. Liesa, J. R. Morones-Ramirez, S. Slomovic, A. Molina, O. S. Shirihai and J. J. Collins, *Sci. Transl. Med.*, 2013, **192**, 1-11.

53. K. Kowalski, J. Skiba, L. Oehninger, I. Ott, J. Solecka, A. Rajnisz, and B. Therrien, *Organometallics*, 2013, **32**, 5766-5773.

54. K. Kowalski, Ł. Szczupak, S. Saloman, D. Steverding, A. Jabłoński, V. Vrček, A. Hildebrandt, H. Lang and A. Rybarczyk-Pirek, *ChemPlusChem*, 2017, **82**, 303-314.

55. G. A. Pankey and L. D. Sabath, *Clin. Infect.Dis.*, 2004, **38**, 864-870.

56. M. A. Kohanski, D. J. Dwyer, B. Hayete, C. A. Lawrence and J. J. Collins, *Cell*, 2007, **130**, 797-810.

57. S. Kalghatgi, C. S. Spina, J. C. Costello, M. Liesa, J. R. Morones-Ramirez, S. Slomovic, A. Molina, O. S. Shirihai and J. J. Collins, *Sci. Transl. Med.*, 2013, **5**, 192-192.

58. H. Van Acker and T. Coenye, *Trends Microbiol.*, 2017, **25**, 456-466.

59. C. A. Fux, S. Wilson and P. Stoodley, *J. Bacteriol.*, 2004, **186**, 4486-4491.

60. E. Gradelski, B. Kolek, D. Bonner and J. J. Fung-Tomc, *Antimicrob.Chemother.*, 2002, **49**, 185-188.

61. C. T. Mascio, J. D. Alder and J. A. Silverman, *Antimicrob. Agents Chemother.*, 2007, **51**, 4255-4260.

62. D. C. Hooper and G. A. Jacoby, *Cold Spring Harb.Perspect. Med.*, 2016, 6:a025320

63. T. Plech, B. Kaproń, A. Paneth, U. Kosikowska, A. Malm, A. Strzelczyk, P. Stączek, Ł. Świątek, B. Rajtar and M. Polz-Dacewicz, *Molecules*, 2015, **20**, 6254-6272.

64. F. Collin, S. Karkare and A. Maxwell, *Appl. Microbiol. Biotechnol.*, 2011, **92**, 479-497.

65. K. Hoshin, A. Kitamura, I. Morrissey, K. Sato, J. Kato and H. Ikeda, *Antimicrob. Agents Chemother.*, 1994, **38**, 2623-2627.

66. M. Kohanski, D. J. Dwyer and J. J. Collins, *Nat. Rev. Microbiol.*, 2010, **8**, 423-435

67. *CrysAlis* CCD and *CrysAlis* RED, *Oxford Diffraction*, Oxford Diffraction Ltd: Yarnton, 2008.

68. R. C. Clark and J. S. Reid. *Acta Crystallogr*., *Sect. A : Found. Crystallogr.,* 1994, ***51***, 887–897.

69. G. M. Sheldrick, *Acta Cryst. Sect. A: Found. Crystallogr.,* 2008, ***64***, 112–122.

70. O.V. Dolomanov, L.J. Bourhis, R.J. Gildea, J.A.K. Howard and H. Puschmann, *J. Appl. Crystallogr.*, 2009, **42**, 339–341.

71. A.L. Spek, *Acta Crystallogr.*, *Sec. D : Biol. Crystallogr.,* 2009, **65**, 148–155.

72. C. F. Macrae, I. J. Bruno, A. Chisholm, P. R. Edgington, P. McCabe, E. Pidcock, L. Rodriguez-Monge, R. Taylor, J. van de Streek and P. A. Wood, *J. Appl. Crystallogr.,* 2008, **41**, 466–470.

73. I. Kubo, K.-I. Fujita, A. Kubo, K.-I. Nihei and T. Ogura, *J. Agric. Food. Chem.* 2004, 52, 3329-3332

74. A. Jabłoński, K. Matczak, A. Koceva-Chyła, K. Durka, D. Steverding, K. Jakubiec-Krześniak, J. Solecka, D. Trzybiński, K. Woźniak, V. Andreu, G. Mendoza, M. Arruebo, K. Kochel, B. Krawczyk, D. Szczukocki and K. Kowalski, *Molecules* 2017, **22**, 2220.

75. H. Hirumi, K. Hirumi, J.J. Doyle and G.A.M. Cross, *Parasitology*, 1980, **80**, 371-782

76. K. Merschjohann, F. Sporer, D. Steverding and M. Wink, *Planta Med.* 2001, **67**, 623-627

77. T. Baltz, D. Baltz, C. Giroud and J. Crockett, *EMBO J.* 1985, **4**, 1273-1277

78. W. Huber and J.C. Koella, *Acta Trop.* 1993, **55**, 257-261

Graphical Abstract

View Article Online
DOI: 10.1039/C9DT03948A

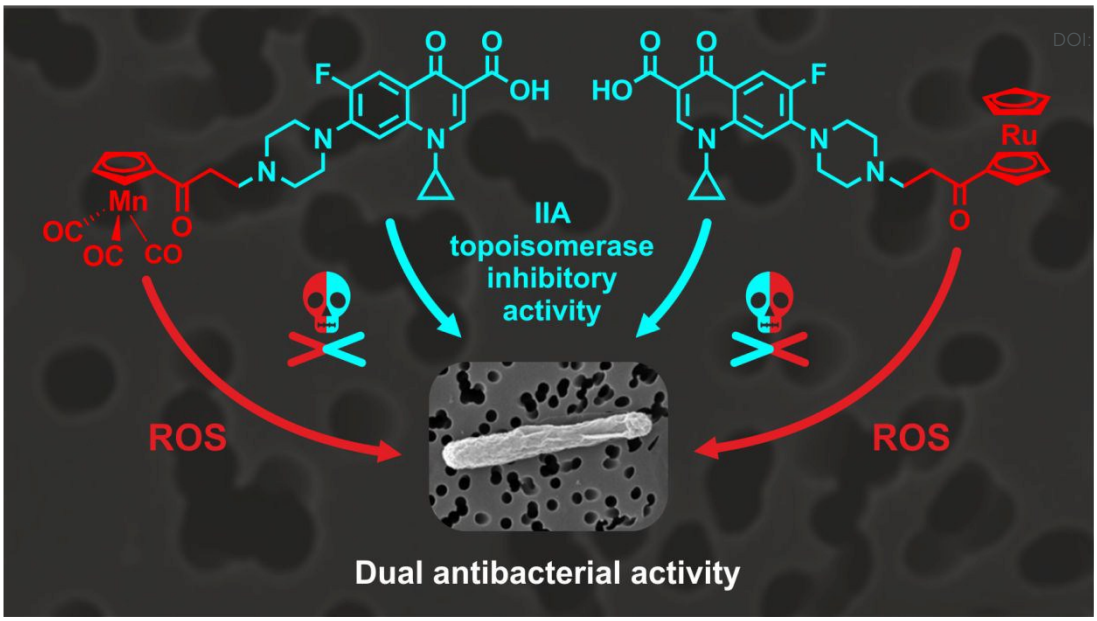

Organometallic ciprofloxacin conjugates were synthesized and showed two mechanisms of antimicrobial activity. The first mechanism involves inhibition of type IIA topoisomerases and the second ROS generation in bacterial cells.